EVALUATION OF THE SORPTION CAPACITY OF A MALEIC ACID COPOLYMER TOWARDS GOLD(III) IONS AND PRODUCTION OF CATALYTICALLY ACTIVE GOLD NANOPARTICLES ON ITS BASE

Cite this: *INEOS OPEN*, **2021**, *4 (4)*, 149–153
DOI: 10.32931/io2119a

Received 23 November 2021,
Accepted 21 December 2021

http://ineosopen.org

N. A. Samoilova* and M. A. Krayukhina

Nesmeyanov Institute of Organoelement Compounds, Russian Academy of Sciences, ul. Vavilova 28, Moscow, 119991 Russia

Abstract

Two spectrophotometric approaches are suggested for the assessment of the concentration of gold(III) cations in an aqueous solution: direct recording of the optical density of gold cations and galvanic substitution of silver atoms in polymer-stabilized silver nanoparticles with gold cations. The sorption capacity of a maleic acid copolymer towards gold cations is estimated. A colloidal composite containing gold nanoparticles is obtained from the polymeric gold salt. The catalytic properties of the resulting polymer-stabilized nanogold are studied in the aerobic oxidation of glucose to gluconic acid.

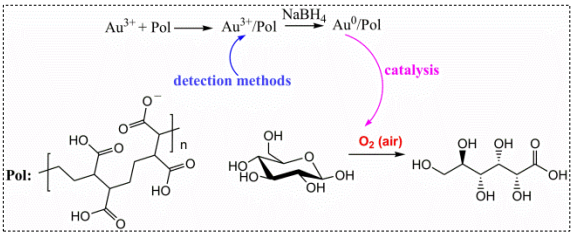

Key words: maleic acid copolymers, determination of gold cations, gold nanoparticles, catalytic activity.

Introduction

In recent years, gold nanoparticles (GNPs) have attracted growing attention owing to a range of unique properties. The ability of the GNPs to exhibit localized surface plasmon resonances allows for creating the electronic and photonic devices, signal converters and amplifiers for different sensor platforms on their base [1–4]. The GNPs find application also in medicine. For example, owing to the biocompatibility, they can be used as drug and gene delivery vehicles, as well as agents for photothermal, photodynamic, and radiotherapy [5, 6]. Furthermore, they can be utilized in diagnostics, radiography, and computed tomography [7–12].

Gold nanoparticles and clusters are also known to serve as efficient catalysts for oxidation of CO, oxidative decomposition of organic compounds, selective oxidation of alcohols, hydrocarbons, saccharides, and other processes [13–18]. In most cases, the GNPs are introduced into solid substrates or porous materials to obtain heterogeneous catalysts. The main drawback of these composites is the lack of stability since these complexes are prone to decomposition during the reaction. Furthermore, special attention should be paid to the possibility of restricted diffusion of the substrates and reagents to the catalytically active centers [19–23].

The homogeneous catalysts containing the GNPs are deprived of these drawbacks [24]. The soluble, colloidal forms of gold nanoparticles represent the complexes of the latter with stabilizing agents used due to the high reactivity of the nanoparticles. The coating agents inhibit the growth of nanoparticles and prevent their aggregation/coagulation during synthesis, application, and storage. The synthesis of nanoparticles can be carried out using different types of stabilizing agents, including surfactants, polymers, dendrimers, cyclodextrins, polysaccharides, *etc*. Polymers are the most frequently used stabilizing agents that not only play a stabilizing role but also facilitate composite dissolution in different media. Moreover, a polymer should contain functional groups which can be used to introduce different auxiliary ligands, in particular, the catalytically active components [25–28].

Earlier we have prepared and explored the colloidal systems bearing silver nanoparticles where the stabilizing polymers were the copolymers of maleic acid [29–31]. The main advantages of the maleic acid (anhydride) copolymers are as follows:

– commercial availability or the possibility of synthesis using the known procedures;

– regular structures (strictly alternating comonomer units);

– the possibility of controlling a hydrophobic-hydrophilic balance among a family of the maleic acid copolymers;

– the water solubility in the form of the maleic acid copolymers;

– the possibility of production of salts with different cations;

– the possibility of modification of the copolymers with different amino- and hydroxy-containing ligands to produce ionic or covalent conjugates.

The goal of this work was to develop convenient approaches for the assessment of the concentration of gold cations in an aqueous solution to study their sorption by a maleic acid copolymer for further nucleation of gold cations and application of the resulting nanocomposite in catalysis.

Results and discussion

The initial step of this work implied the investigation of the sorption of Au^{3+} ions by a maleic acid copolymer using the copolymer of maleic acid with ethylene (EMA) as an example and evaluate the sorption capacity of this copolymer towards

gold cations since the real binding degrees of metal cations by copolymers always differ from the calculated values, which is connected with the cation nature, ionization degree of the polyanion carboxy groups, and the polymer conformation in solution [32, 33].

Earlier the detection of gold cations in solution has been accomplished by the relatively laborious methods: using a gold-specific sensor protein [34], an optical mesocaptor with an immobilized probe, namely, 6-hydroxy-5-(4-sulfophenylazo)-2-napthtalenesulfonic acid disodium salt [35], a chemosensor for Au(III) bearing rhodamine B fluorophore on the chitosan nanoparticle surface [36] or a chelating agent, namely, hydroxypyridinone 3,4,3-LI(1,2-HOPO) [37].

In this work, the binding degree of gold cations (Au^{3+}) by the chosen copolymer was estimated using the dialysis method. To follow the course of the sorption of gold cations by the copolymer, two simple spectrophotometric approaches were suggested: the direct detection of the changes in the absorbance of Au^{3+} at 290 nm (approach A) and registration of the changes in the absorbance of silver nanoparticles in the range of the surface plasmon resonance maximum at 410 nm during the galvanic oxidation of silver nanoparticles with gold cations from the taken samples (approach B). In the latter case, the working solution of the nanosilver was the ethylene–maleic acid copolymer bearing silver nanoparticles (EMA/Ag^0) obtained and characterized by our research group earlier [29]. Figure 1 depicts the TEM micrograph of the EMA/Ag^0 sample. The diameter of silver particles in this sample was 1.5 ± (0.2–0.3) nm.

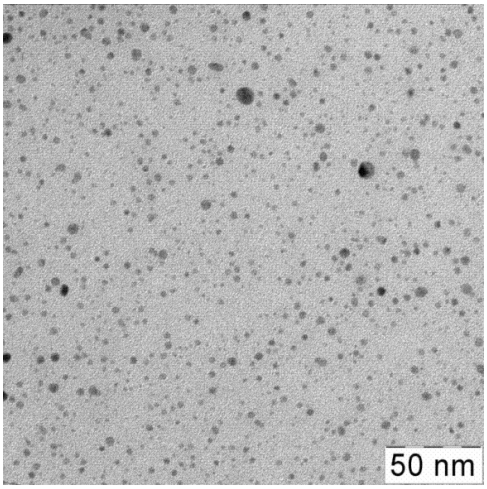

Figure 1. TEM micrograph of the EMA/Ag^0 particles.

The galvanic substitution of silver atoms in silver nanoparticles for the gold ones occurs owing to a difference in the standard electrode potentials of silver and gold (1.68 V for Au and 0.80 V for Ag) [38].

The calibration equations for the suggested approaches are presented in Figs. 2 and 3. Figure 3 includes the recalculation of the concentration of gold cations according to the molar ratios of the cations and atoms in the following equation: $3Ag^0 + Au^{3+} = 3Ag^+ + Au^0$. It should also be noted that the first approach implies the direct measurement of the concentration of gold cations in the working solution, while in the second case, an aliquot of the working solution is taken and diluted with the nanosilver solution (see Experimental).

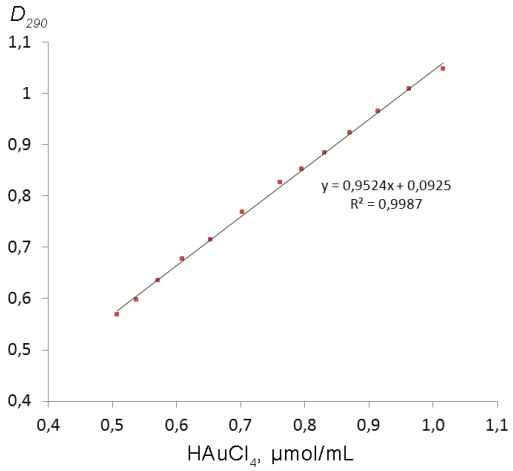

Figure 2. Calibration line for the first approach (A).

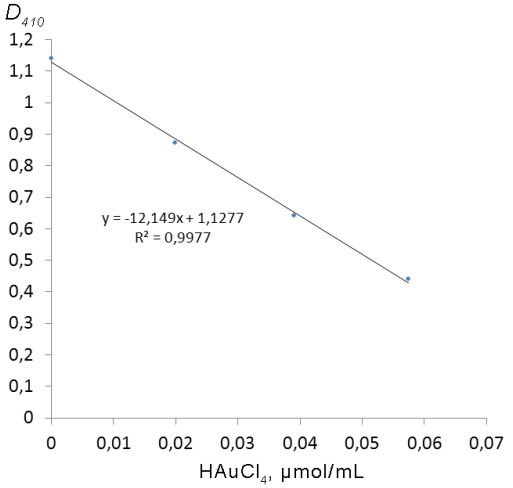

Figure 3. Calibration line for the second approach (B).

The copolymer capacity towards gold cations was studied at pH = 6 and 10. Figure 4 shows typical changes in the optical density of the control solutions of gold (Fig. 4a) and nanosilver (Fig. 4b) cations for the EMA sample in time registered by two methods at pH = 6. In Fig. 4a, the concentration of gold cations in the external solution naturally reduces until the polymer saturation with gold cations in the internal solution. In Fig. 4b, the concentration of the nanosilver test solution in the samples grows with the migration of gold cations to the polymer solution, *i.e.*, a lower number of gold cations enters the reaction with silver nanoparticles.

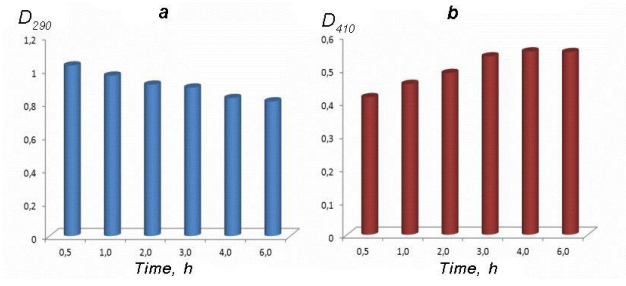

Figure 4. Changes in the optical density of the test solutions during the determination of the EMA capacity towards gold cations in time: approach A (***a***), approach B (***b***).

The sorption almost comes to completion in 4 h. The degree of carboxy group substitution in the maleic acid copolymer at this pH was 18.4 mol % according to approach A and 19.0 mol % according to approach B. At pH = 10, this value composed 30–36% for both of the methods (a confidence interval of the measurements was 20%). The direct registration of gold cations in an aqueous solution by measuring the optical density at the plasmon resonance maximum is simpler and does not require additional reagents and manipulations. However, in this case, some shift of the plasmon resonance peak with a change of the solution pH should be taken into account.

The resulting copolymer–gold cation complex was converted to the copolymer/nanogold composite. It was found that an optimal ratio of auric acid to the copolymer ($HAuCl_4$/EMA, mol/mol) during gold nucleation in the presence of an excess of sodium borohydride was 14–20/1, which did not exceed the above-mentioned capacity of the copolymer towards gold cations. This range of ratios provided for the colloidal solutions stable for a long time (no less than one month). According to the optical spectroscopic data, a peak of the surface plasmon resonance for the GNPs corresponds to 520 nm (Fig. 5).

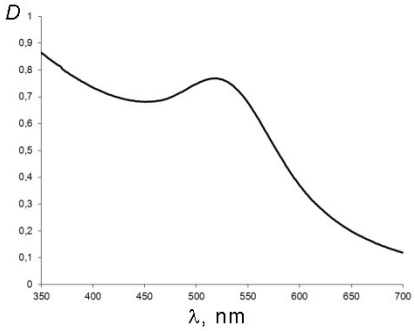

Figure 5. Optical spectrum of the EMA/Au^0 sample.

According to the TEM data, the shape of the GNPs in the sol samples was close to spherical. The particle diameter was 3.5 ± 0.5 nm (Fig. 6).

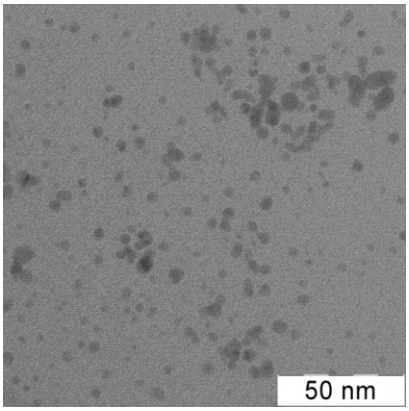

Figure 6. TEM micrograph of the EMA/Au^0 particles.

The catalytic properties of the resulting nanocomposite were studied in the aerobic oxidation of glucose to gluconic acid (GA). The latter represents a pharmaceutical product and food additive E574. The glucose oxidation was monitored by measuring the amount of released hydrogen peroxide, which was defined by the reaction of the latter with the iodide anion in the presence of ammonium molybdate used as a catalyst [39].

$$C_6H_{12}O_6 + O_2 + H_2O \rightarrow C_6H_{12}O_7 + H_2O_2$$

$$I^{-1} + O^{-1} \rightarrow I^0 + O^{-2}$$

To evaluate the efficiency of glucose oxidation by this method, we used an alkaline medium since gold was shown to display the highest performance just in this medium [40]. The activity of the EMA/Au^0 colloidal catalyst in the aerobic oxidation of glucose was found to be 32.5 mmol h^{-1} g^{-1} for the catalyst or 7.4 mmol h^{-1} g^{-1} for gold. The activity of this catalyst calculated per a weight fraction of the catalyst was about 2 times higher than that of Au/Al_2O_3 and Au/C also used in the aerobic glucose oxidation (T = 60 °C, pH = 9) [41].

The catalyst obtained can be precipitated after the reaction in the form of a calcium salt. In this case, the target product, calcium gluconate, remains in solution, while the catalyst can be separated by filtration, dissolved in an alkaline medium, and reused.

Experimental

Materials

The copolymer of maleic acid and ethylene was obtained by the hydrolysis (*via* dissolution in deionized water followed by freeze drying) of an alternating copolymer of maleic anhydride and ethylene (Monsanto, USA, $M_w = 2.5 \times 10^4$). $NaBH_4$, $AgNO_3$, NaCl, NaOH, KI, $(NH_4)_2MoO_4$, anhydrous $CaCl_2$ (Reakhim, all of reagent grade), glucose, and $HAuCl_4 \cdot 3H_2O$ (Sigma-Aldrich) were purchased from commercial sources and used without purification. The colloidal solution of nanosized silver EMA/Ag^0 was prepared according to the published procedure [29].

Methods

Methods for the analysis of the samples. The medium pH was measured with a Fisher Scientific 300 403.1 pH meter (USA). The optical spectra were registered on a Hitachi U-5100 spectrophotometer (Japan) in glassy cuvettes with 0.2 and 1 cm pathlengths. The TEM images of the resulting GNPs were obtained with a LEO 912 AB transmission electron microscope (OMEGA, Karl Zeiss, Germany) equipped with a magnetic omega spectrometer with an energy filter integrated directly into the optical system of the instrument. The accelerating voltage was 100 kV, the magnification ranged from 80× to 500000×, and the image resolution varied within 0.2–0.34 nm. For investigations, a drop of the solution under consideration was applied to a 3 mm copper network coated with formvar and dried under vacuum. The size distribution of the GNPs was calculated from the analysis of the resulting images using at least 100 particles.

Investigation of the binding of Au^{3+} cations with the EMA copolymer. The binding of gold cations by the mentioned copolymer was studied by the dialysis method. A cell with a membrane (Spectrapor, M.W. 6000–8000) was charged with a solution of EMA (1.1 mL, 0.007 M) and placed into an external solution containing $HAuCl_4$ (8.0 mL, 0.001 M). The system was stirred at room temperature; the sorption of metal cations was

controlled spectrophotometrically taking the samples of the external solution in certain time periods.

Approach A. The spectrophotometric analysis of the samples (0.5 mL) was carried out using quartz cuvettes with l = 0.2 cm at the wavelength of 290 nm.

Approach B. The galvanic substitution of silver atoms in silver nanoparticles with gold atoms was accomplished upon the addition of 30 μL samples of the external solution to a solution of EMA/Ag^0 (470 μL, 0.05 M). The spectrophotometric analysis of the samples was performed after mixing the solutions using quartz cuvettes with l = 0.2 cm at the wavelength of 410 nm.

Synthesis of the GNPs. The colloidal solutions of nanosized gold were obtained by the borohydride reduction of a metal salt at room temperature in the presence of the maleic acid copolymer according to the published procedure [29]. The required amount of the freshly prepared solution of $HAuCl_4 \cdot 3H_2O$ (0.1 M) (14 mol % of Au) was added to the freshly prepared solution of EMA in double distilled water (0.006 M, pH = 3) under vigorous stirring; in 0.5 h, the freshly prepared solution of $NaBH_4$ (0.1 M) was added to the polymeric salt under vigorous stirring using a 7-fold excess relative to gold ions. The reaction mixture was stirred at room temperature for a day. The dried EMA/Au^0 samples were obtained after the dialysis (or ultrafiltration) of the reaction mixture followed by freeze drying (–550 °C, 0.05 mbar).

Catalytic experiments. A cell thermostated at 50 °C was charged with 2 mL of 0.05 M Tris-buffer (pH = 9) bearing 2 mg of the catalyst. Then, 0.1 mL of a solution of glucose (1.8 mg/mL) was added. The reaction was performed by passing air through the mixture (500 mL min^{-1}) for 4 h.

The content of hydrogen peroxide resulting from the reaction was analyzed by the reaction of the samples with 0.04 mL of 10% KI solution in the presence of the catalyst (0.02 mL of 0.02 M solution of $(NH_4)_2MoO_4$) (released I_2 was registered at 360 nm) according to the published procedure [39]. The glucose conversion over this period of time was 72%.

Conclusions

Hence, simple spectrophotometric approaches were suggested for the analysis of the content of Au^{3+} cations in aqueous solutions. The capacity of the maleic acid copolymer towards gold cation was evaluated. The suggested approaches can be further extended for analytical control of the content of this cation in different mixtures to study the binding of gold cations with a broad spectrum of sorbents and carriers. The polymeric gold salts obtained in this work were converted to composites bearing gold nanoparticles. The catalytic properties of the polymer-stabilized nanogold in the form of a colloidal solution were studied in the aerobic oxidation of glucose into gluconic acid. This catalyst appeared to be efficient and can be recycled. The resulting composites may find application in other catalytic transformations, biosensing, and medical diagnostics.

Acknowledgements

The authors are grateful to Dr. S. S. Abramchuk for the help with the TEM analysis.

This work was performed with financial support from the Ministry of Science and Higher Education of the Russian Federation using the equipment of the Center for Molecular Composition Studies of INEOS RAS.

Corresponding author

* E-mail: samoilova@ineos.ac.ru. (N. A. Samoilova)

References

1. J. H. Teichroeb, J. A. Forrest, V. Ngai, L. W. Jones, *Eur. Phys. J. E: Soft Matter Biol. Phys*., **2006**, *21*, 19–24. DOI: 10.1140/epje/i2006-10040-2
2. S. Link, M. A. El-Sayed, *Annu. Rev. Phys. Chem*., **2003**, *54*, 331–366. DOI: 10.1146/annurev.physchem.54.011002.103759
3. W. Zhao, M. A. Brook, Y. Li, *ChemBioChem*, **2008**, *9*, 2363–2371. DOI: 10.1002/cbic.200800282
4. M. Y. Sha, H. Xu, S. G. Penn, R. Cromer, *Nanomedicine*, **2007**, *2*, 725. DOI: 10.2217/17435889.2.5.725
5. R. Bhattacharya, P. Mukherjee, *Adv. Drug Delivery Rev*., **2008**, *60*, 1289–1306. DOI: 10.1016/j.addr.2008.03.013
6. S. J. Amina, B. A. Guo, *Int. J. Nanomedicine*, **2020**, *15*, 9823–9857. DOI: 10.2147/IJN.S279094
7. X. Hu, Y. Zhang, T. Ding, J. Liu, H. Zhao, *Front. Bioeng. Biotechnol.*, **2020**, *8*, 990. DOI 10.3389/fbioe.2020.00990
8. N. Elahi, M. Kamali, M. H. Baghersad, *Talanta*, **2018**, *184*, 537–556. DOI: 10.1016/j.talanta.2018.02.088
9. Y.-C. Yeh, B. Creran, V. M. Rotello, *Nanoscale*, **2012**, *4*, 1871–1880. DOI: 10.1039/C1NR11188D
10. N. Nashat, Z. Haider, *Int. J. Nanomater. Nanotechnol. Nanomed*., **2021**, *7*, 019–025. DOI: 10.17352/2455-3492.000040
11. K. Nejati, M. Dadashpour, T. Gharibi, H. Metllatyar, A. Akbarzaden, *J. Cluster Sci.*, **2021**. DOI: 10.1007/s10876-020-01955-9
12. M. Sengani, A. M. Grumezescu, V. D. Rajeswari, *OpenNano*, **2017**, *2*, 37–46. DOI: 10.1016/j.onano.2017.07.001
13. M. H. Naveen, R. Khan, J. H. Bang, *Chem. Mater.*, **2021**, *33*, 7595–7612. DOI: 10.1021/acs.chemmater.1c02112
14. R. Jin, G. Li, S. Sharma, Y. Li, X. Du, *Chem. Rev*., **2021**, *121*, 567–648. DOI: 10.1021/acs.chemrev.0c00495
15. M. Stratakis, H. Garcia, *Chem. Rev*., **2012**, *112*, 4469–4506. DOI: 10.1021/cr3000785
16. S. A. C. Carabineiro, *Front. Chem*., **2019**, *7*, 702. DOI: 10.3389/fchem.2019.00702
17. T. Tabakova, *Front. Chem*., **2019**, *7*, 517. DOI: 10.3389/fchem.2019.00517
18. Y. Zhang, X. Cui, F. Shi, Y. Deng, *Chem. Rev*., **2012**, *112*, 2467–2505. DOI: 10.1021/cr200260m
19. M. Egi, K. Azechi, S. Akai, *Adv. Synth. Catal*., **2011**, *353*, 287–290. DOI: 10.1002/adsc.201000753
20. A. Corma, C. González-Arellano, M. Iglesias, F. Sánchez, *Appl. Catal., A*, **2010**, *375*, 49–54. DOI: 10.1016/j.apcata.2009.12.016
21. M. Raducan, C. Rodríguez-Escrich, X. C. Cambeiro, E. Escudero-Adán, M. A. Pericàs, A. M. Echavarren, *Chem. Commun.*, **2011**, *47*, 4893–4895. DOI: 10.1039/C1CC10293A
22. M. P. de Almeida, S. A. C. Carabineiro, *ChemCatChem*, **2012**, *4*, 18–29. DOI: 10.1002/cctc.201100288
23. G. Villaverde, A. Corma, M. Iglesias, F. Sánchez, *ACS Catal*., **2012**, *2*, 399–406. DOI: 10.1021/cs200601w
24. G. I. Dzhardimalieva, A. K. Zharmagambetova, S. E. Kudaibergenov, I. E. Uflyand, *Kinet. Catal.*, **2020**, *61*, 198–223. DOI: 10.1134/S0023158420020044
25. R. Javed, M. Zia, S. Naz, S. O. Aisida, N. ul Ain, Q. Ao, *J. Nanobiotechnol.*, **2020**, *18*, 172. DOI: 10.1186/s12951-020-00704-4
26. M. Das, K. H. Shim, S. S. A. An, D. K. Yi, *Toxicol. Environ. Health Sci*., **2011**, *3*, 193–205. DOI: 10.1007/s13530-011-0109-y

27. D. Cabuzu, A. Cirja, R. Puiu, A. M. Grumezescu, *Curr. Top. Med. Chem.*, **2015**, *15*, 1605–1613. DOI: 10.2174/1568026615666150414144750
28. W. Cai, T. Gao, H. Hong, J. Sun, *Nanotechnol. Sci. Appl.*, **2008**, *1*, 17–32. DOI: 10.2147/NSA.S3788
29. N. Samoilova, E. Kurskaya, M. Krayukhina, A. Askadsky, I. Yamskov, *J. Phys. Chem. B*, **2009**, *113*, 3395–3403. DOI: 10.1021/jp806683m
30. N. A. Samoilova, M. A. Krayukhina, O. V. Vyshivannaya, I. V. Blagodatskikh, D. A. Popov, N. M. Anuchina, I. A. Yamskov, *Russ. Chem. Bull.*, **2018**, *67*, 1010–1017. DOI: 10.1007/s11172-018-2172-x
31. N. Samoilova, M. Krayukhina, A. Naumkin, N. Anuchina, D. Popov, *New J. Chem.*, **2021**, *45*, 14513–14521. DOI: 10.1039/D1NJ02478G
32. P. L. Dubin, U. P. Strauss, *J. Phys. Chem.*, **1970**, *74*, 2842–2847. DOI: 10.1021/j100708a020
33. U. P. Strauss, B. W. Barbieri, G. Wong, *J. Phys. Chem.*, **1979**, *83*, 2840–2843. DOI: 10.1021/j100485a007
34. W. Wei, T. Zhu, Y. Wang, H. Yang, Z. Hao, P. R. Chen, J. Zhao, *Chem. Sci.*, **2012**, *3*, 1780–1784. DOI: 10.1039/C2SC01119K
35. E. A. Elshehy, S. A. El-Safty, M. A. Shenashen, M. Khairy, *Sens. Actuators*, *B*, **2014**, *203*, 363–374. DOI: 10.1016/j.snb.2014.06.055
36. J. Liu, W. Liu, M. Xu, B. Wang, Z. Zhou, L. Wang, *Sens. Actuators*, *B*, **2016**, *233*, 361–368. DOI: 10.1016/j.snb.2016.04.086
37. R. M. Pallares, K. P. Carter, S. E. Zeltmann, T. Tratnjek, A. M. Minor, R. J. Abergel, *Inorg. Chem.*, **2020**, *59*, 2030–2036. DOI: 10.1021/acs.inorgchem.9b03393
38. S. Megarajan, R. K. Kamlekar, P. S. Kumar, V. Anbazhagan, *New J. Chem.*, **2019**, *43*, 18741–18746. DOI: 10.1039/C9NJ04289J
39. H. V. Malmstadt, S. I. Hadjiioannou, *Anal. Chem.*, **1962**, *34*, 455–458. DOI: 10.1021/ac60184a004
40. P. Quaino, N. B. Luque, R. Nazmutdinov, E. Santos, W. Schmickler, *Angew. Chem., Int. Ed.*, **2012**, *51*, 12997–13000. DOI: 10.1002/anie.201205902
41. I. V. Delidovich, B. L. Moroz, O. P. Taran, N. V. Gromov, P. A. Pyrjaev, I. P. Prosvirin, V. I. Bukhtiyarov, V. N. Parmon, *Chem. Eng. J.*, **2013**, *223*, 921–931. DOI: 10.1016/j.cej.2012.11.073